OVERSTRAIN OF HIGH-STRENGTH C[illegible]ND CYLINDERS O[illegible]NTERMEDIATE DIAM[illegible]RATIO

T. E. Davidson, C. S. Barton,* A. N. E[illegible]s, D. P. Kendall

Watervliet Arsenal, Watervlie[illegible] York

Abstract—Those associated with the pressure vessel [illegible] have long been interested in means for increasing the elastic load carrying capac[illegible] of thick-wall cylinders. Over the years, such techniques as wire wrapping, bore quenching and the more common jacketing and autofrettage have been utilized.

Recent requirements in the pressure vessel and weapons fields now make it necessary to consider means for even further increasing the elastic load carrying capacity of cylinders fabricated from high-strength materials. This paper describes the results of an experimental program associated with the application of the autofrettage principle to materials in the 160,000–190,000 psi yield strength level and diameter ratio range of 1.4–2.4.

Data are presented for the elastic breakdown and full overstrain pressure as a function of diameter ratio and compared to that theoretically predicted based on the Tresca and von Mises yield criteria.

Data are also presented for the permanent enlargement and enlargement ratio associated with the complete overstrain condition.

Also presented is a system of simplified equations for the stresses and strains in both the elastic and plastic regions of an overstrained open-end cylinder. These equations are based on an approximation of the von Mises yield criterion and show very good agreement with the experimental results.

LIST OF SYMBOLS

P = pressure
ϵ = unit strain
σ = stress
σ_y = yield stress
r = variable radius
a = inside radius
b = outside radius
ρ = radius of elastic–plastic interface
W = diameter ratio, b/a
μ = Poisson's ratio
E = Young's modulus of elasticity
PF = pressure factor, P/σ_y
SF = strain factor, $\epsilon E/\sigma_y$

* Now at Brigham Young University, Provo, Utah.

u = radial displacement
PER = permanent enlargement ratio

Subscripts
t = tangential
r = radial
z = longitudinal
p = plastic region
e = elastic region
o = 100 percent overstrain condition

INTRODUCTION

The requirements for pressure vessels of high elastic load carrying capacity is rapidly increasing as evidenced by the rapid advancements in such fields as chemical processing and hydrostatic compacting. Similarly, in such fields as cannon, there is a constant aim towards increasing the strength to weight ratio of weapons. Along with this trend towards higher pressures in these and other fields, the design and fabrication of pressure vessels becomes increasingly difficult. A point is reached where it is no longer feasible to simply increase the diameter ratio and/or the basic material strengths and it becomes necessary to consider other means of increasing the elastic load carrying capacity. The most common techniques for increasing the elastic load carrying capacity are jacketing, wire wrapping and autofrettage. All of these techniques are based on the use of induced residual stresses to counteract the operating stresses. Autofrettage, however, is the most efficient. It has been the purpose of the work summarized in this paper to study the application of the autofrettage principle to pressure vessels fabricated from current high strength materials.

Autofrettage is a process by which a favorable residual stress distribution is produced by subjecting the cylinder to an internal pressure of sufficient magnitude to cause plastic flow in part or all of the cylinder wall. When the pressure is released, residual stresses are set up which are compressive near the bore changing to tensile towards the outside surface. These residual stresses oppose the operating stresses, thus increasing the elastic load carrying capacity of the vessel.

Several investigators have studied the theoretical solution in terms of the stresses and strains associated with the overstrain of thick-wall cylinders. These solutions, however, are primarily based on the Tresca yield criterion and, although simple by comparison, they are inherently inaccurate as compared to those based on the von Mises yield criterion. Unfortunately, however, the use of the von Mises criterion results in very complex relationships that often cannot be obtained in closed form.

The experimental study of the overstrain of thick-wall cylinders in the past has been primarily limited to low-strength materials by today's standards. Consequently, much of the data is inaccurate and incomplete when applied to current high strength materials.

This paper summarizes a portion of the results of an experimental program associated with the study of the overstrain of thick-wall cylinders in the diameter ratio range of 1.4–2.4 and nominal yield strength level of 165,000 psi. Experimental data are presented for the pressure required for, and the displacements associated with, the 100 percent overstrain condition. Using empirical relationships, the solution for the open-end cylinder condition using the von Mises criterion is presented. Simplified relationships are given and compared to the experimental data for both the stresses and displacements in the plastic and elastic portion.

In addition to those subjects covered within this paper, other phases of the study of overstrained thick-wall cylinders are under way and will be reported at a later date. Included are experimental determinations of the residual stress distribution, effects of material removal and temperature on the plastic strength, and progressive stress damage studies.

DESCRIPTION OF TESTS AND APPARATUS

Test Specimens

The specimen geometry consisted of a common initial 1-in. bore diameter with a length of 11 in. This length was determined to be great enough to overcome end effects in the largest diameter investigated.

All specimens were obtained from 4340 steel billets 80 in. long and 4.5 in. in diameter which were gun drilled and cut into two 40 in. lengths. These lengths were heat treated by austenitizing at 1525°F, oil quenching in the longitudinal direction and tempering at 1075°F ± 25° with a resultant nominal yield strength of 165,000 psi. Each heat treated bar was then finish reamed to 1 in. I.D. and cut to obtain three 11 in. specimens. The remaining 7 in. of material provided tensile and charpy specimens.

Restraining Containers

Preliminary experimentation was conducted using several specimens, ranging in diameter ratio from 1.4 to 2.4, to determine the uniformity of strain along the specimen length. Due to the natural inhomogeneity of material, particularly at this high strength level, large variations in plastic dilation were noted, both along the length and circumferentially. Therefore, to insure uniform deformation throughout, external restraining containers were utilized. These containers were split at the half-length point and recessed to allow the application of strain gages to the specimen surface as shown in Fig. 1.

FIG. 1. Specimen and container arrangement.

Pressure Seals

The seal configuration used, as shown in Fig. 2, was of the unsupported area type consisting of an "O" ring and an annealed 1020 steel ring that is forced [illegible] an inclined plane by the internal pressure. This configuration was considered as the simplest and most trouble-free over the large range of pressures, temperatures, bore enlargements, and diameter ratios encountered in this investigation.

Test Apparatus

The pressure source as shown in Fig. 3 was a 200,000 psi 10 in³/min intensifier type pumping system manufactured by the Harwood Engineering Company. This system has an intensification ratio of 100:1 with a low pressure source of 2000 psi and a charging pressure of 10,000 psi.

Pressures were measured with a Manganin cell and a Wheatstone bridge. This Manganin pressure measurement system was calibrated on a controlled clearance piston gage which utilizes a known weight supported on a free piston of known area. In this device the unknown pressure, which the Manganin cell measures, is introduced into the bottom of the cylinder and

the piston floated. From the known weight supported by the piston of a specified area, the pressure can be determined to an accuracy of 0.1 percent.

The tangential strain at the outside surface during the application of pressure was measured by 2 SR-4 type strain gages attached to the outside surface of the specimen at the midlength and diametrically opposed. An SR-4 strain

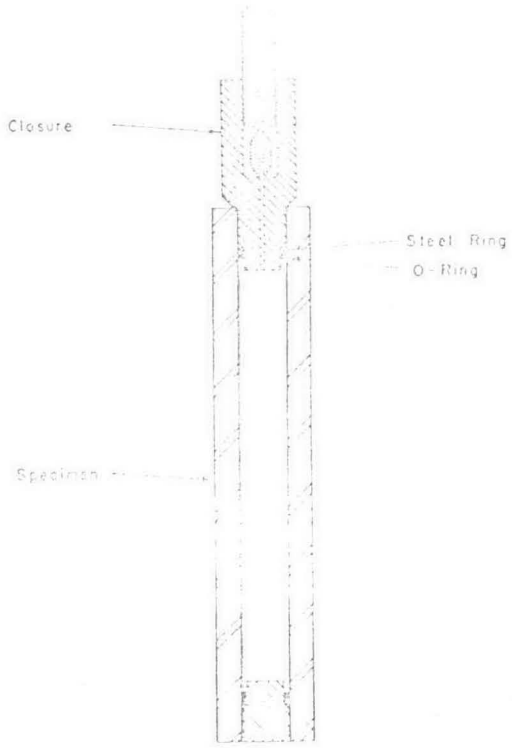

FIG. 2. Pressure seal configuration.

indicator was used on most tests for measuring the strain. A photograph of the physical strain measurement setup is shown in Fig. 4. Supplemental data was obtained using a Moseley Model 2S X-Y recorder. This recorder simultaneously measured and plotted outside surface strain and pressure. It was calibrated by the use of an accurate shunt resistance in one arm of a 4-arm bridge.

The overall experimental accuracy depended upon the Manganin cell and Wheatstone bridge in the pressure measurement system, and strain gages, SR-4 indicator, X-Y recorder and associated strain recording equipment in the strain-measurement circuit. The estimated error, including the human

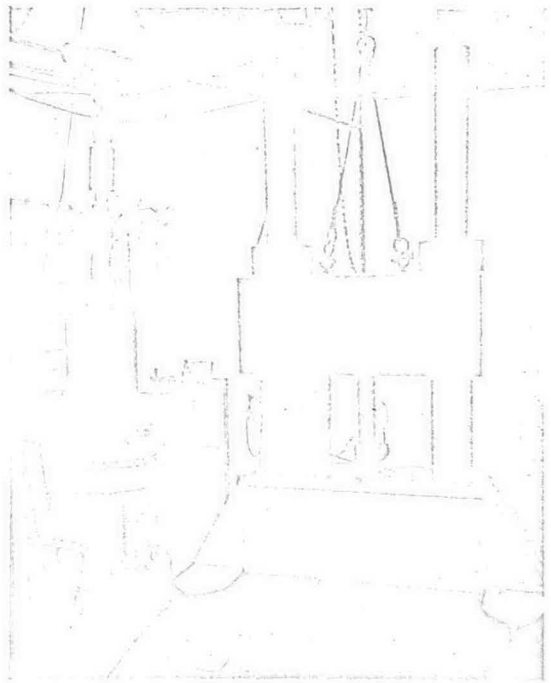

FIG. 3. 200,000 psi testing system.

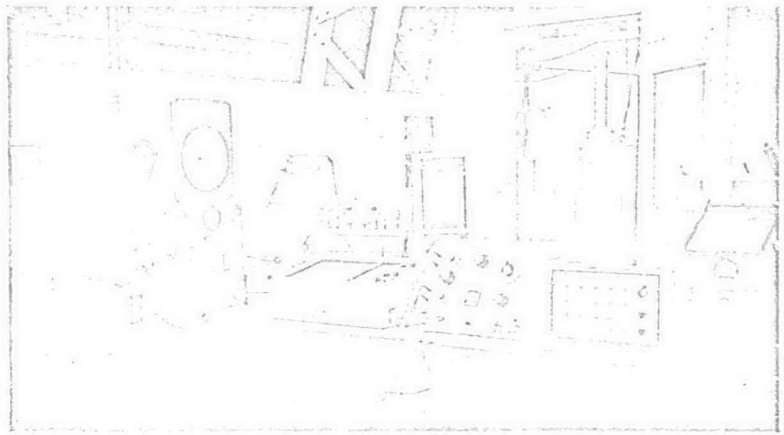

FIG. 4. Pressure and strain measurement equipment.

element, was approximately 1 percent in the pressure measuring system and 4 per cent in the strain measurement circuit.

Test Procedure

As previously stated, all the data in this study was obtained from cylinders laterally supported by restraining containers during autofrettage. The predicted percent bore enlargement was controlled by the outside diameter of the specimen, thus controlling the subsequent expansion of each specimen. In order to determine when the desired percent overstrain was obtained, the container was strain gaged using SR-4 type, A-7 gages tangentially directed and diametrically opposed at intervals along the length of the container. When a small, but substantial reading (generally between 100 and 200 μin./in.), was obtained on all container gages, it was assumed that the specimen had uniformly contacted the container and uniform plastic flow achieved.

Strain readings from the 2 tangential gages on the midsection of the specimen were recorded at appropriate intervals of induced internal pressure. From these data, plots of internal pressure vs. outside surface strain from both tangential strain gages were made for increasing and decreasing pressure. On a few tests, longitudinal strain was measured by cementing longitudinally oriented strain gages.

Physical dimensions of the bore, external diameter, and length were measured, before and after autofrettage, utilizing screw micrometers and dial bore gages to an accuracy of $\pm$ 0.0002 in.

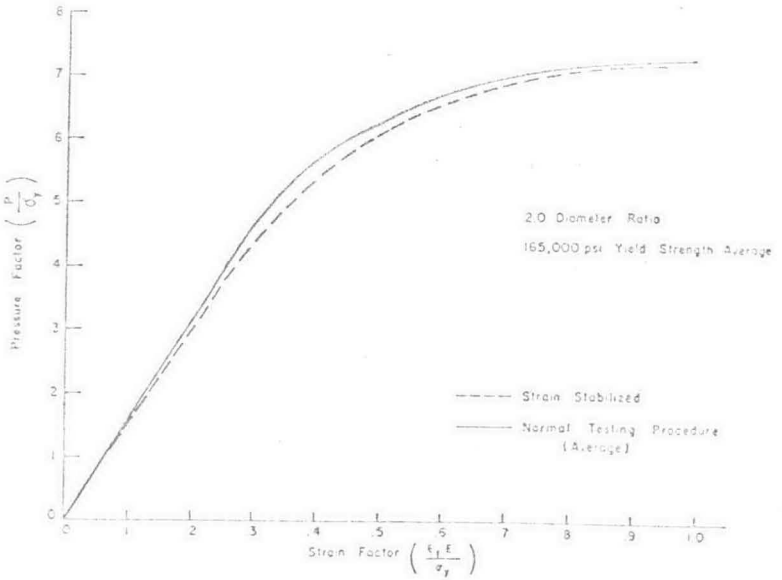

FIG. 5. Pressure factor vs. strain factor showing effect of strain stabilization.

During the tests, the delay or "stabilization" period for the measurement of the increment of strain produced by a pressure change was maintained at approximately 30 sec per reading. Some specimens were tested, however, allowing complete strain "stabilization" at each pressure increment. As shown in Fig. 5, the use of the 30 sec "stabilization" period did not significantly change the results as derived from the pressure-strain data and it allowed the testing of a large number of cylinders in a limited period of time.

RESULTS AND DISCUSSION

End condition Analysis

In the pressure seal configuration [illegible]ed, the seal was not mechanically fixed to the tube or cylinder. How[illegible]since the steel ring moves up the

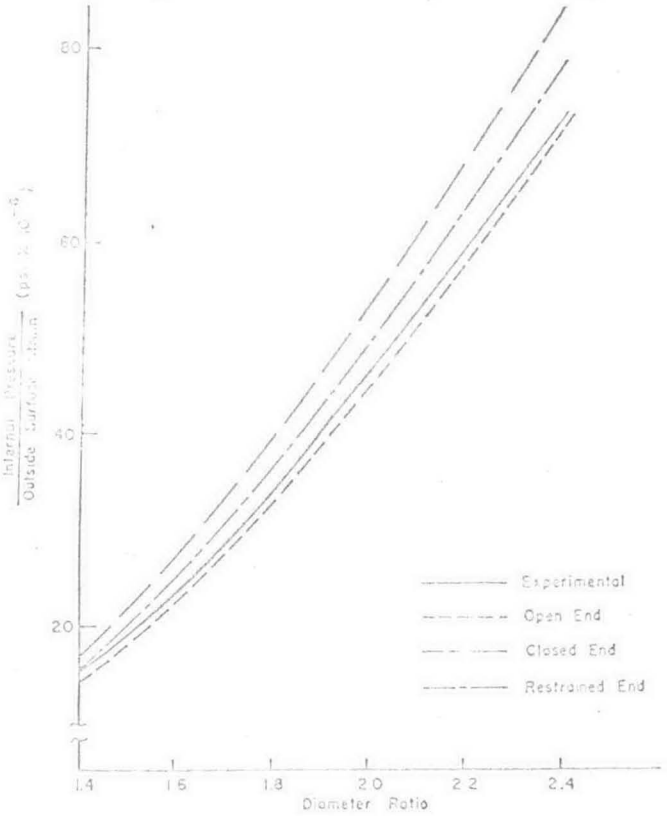

FIG. 6. Slope in the elastic range of internal pressure—outside surface strain curve vs. diameter ratio.

inclined plane of the seal head, there is a tensile longitudinal stress induced in the cylinder from the frictional forces between the ring and the inner cylinder wall. As will be shown, however, this stress is of low enough magnitude that

the results obtained more closely approximated the open end than closed end condition.

Using Hookes' Law and the Lamé equations for elastic stresses in thick-walled cylinders, it can be shown that the slopes of the pressure—outside surface strain curve in the elastic region for the various end conditions are:

1. Closed end $$\frac{P}{\epsilon_{tb}} = \frac{W^2 - 1}{2 - \mu}$$
2. Open end $$\frac{P}{\epsilon_{tb}} = \frac{W^2 - 1}{2}$$
3. Restrained end $$\frac{P}{\epsilon_{tb}} = \frac{W^2 - 1}{2(1 - \mu^2)}$$

Figure 6 shows a plot of these equati[illegible]lus a curve showing [illegible]verage values obtained experimentally. From t[illegible]ure it is seen that [illegible]ysical condition encountered in this experime[illegible]rogram correlates [illegible]with the open end condition.

Elastic Breakdown

The plot of internal pressure versus outside surface strain is linear [illegible]to initial yield or elastic breakdown at the bore. The experimental values for the elastic breakdown pressure were averaged for each diameter ratio and plotted in Fig. 7 as a fu[illegible]n of pressure factor vs. diameter ratio. For

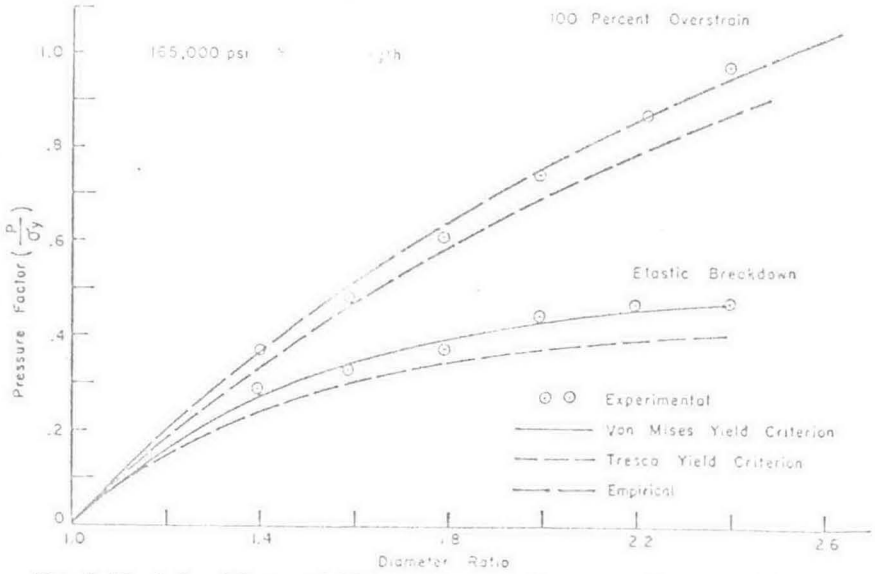

FIG. 7. Elastic breakdown and 100 percent overstrain pressure factor vs. diameter ratio.

comparison, the theoretical elastic breakdown pressure factor, based on the von Mises and Tresca yield criteria for the open end condition, are also shown. Based on the von Mises yield criterion and assuming $\sigma_z = 0$, elastic breakdown occurs when:

$$PF = \frac{W^2 - 1}{\sqrt{(3W^4 + 1)}} \tag{1}$$

From the Tresca yield criterion elastic breakdown is:

$$PF = \frac{W^2 - 1}{2W^2} \tag{2}$$

As can be seen from the figure, there is close correlation between the experimentally determined and the theoretical von Mises elastic breakdown condition.

100 Percent Overstrain

When the internal pressure exceeds the elastic breakdown pressure, the elastic-plastic interface moves from the bore towards the outside diameter. This movement is a function of the internal pressure, yield strength, diameter

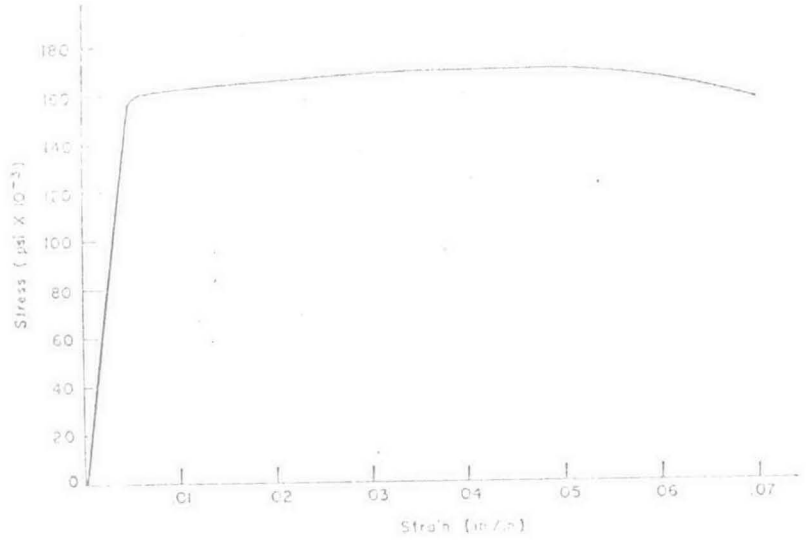

FIG. 8. Stress-strain diagram.

ratio and the strain hardening capabilities of the material. The strain hardening of this material at the yield-strength level considered is small, as shown in Fig. 8 which is a tensile stress-strain diagram for the material used in this program. As can be seen from the figure, for purposes of calculation and

interpretation of the experimental results, the assumption of a elastic-perfectly plastic material is valid.

The exterior surface of an open end cylinder subjected to internal pressure is in a condition of uniaxial stress since σ_r and σ_z are zero. Therefore, the condition of 100 percent overstrain may be defined as that at which the outside surface strain equals the strain associated with the yield stress of the material in uniaxial tension or

$$\epsilon_{\theta_0} = \frac{\sigma_y}{E} \tag{3}$$

The pressure required to produce this condition (P_0) was experimentally determined for the specimens tested. It should be noted that, since most of the specimens were designed for greater than 100 percent overstrain, there was use of no contact between the specimen and container at the 100 percent overstrain condition. These values of P_0 were converted to pressure factor, and all values for the same diameter ratio were averaged and plotted in Fig. 7. These data may be represented by an empirical relationship:

$$P_0 = 1.08\, \sigma_y \log W \tag{4}$$

Weigle[1] gives the following equation for the 100 percent overstrain pressure based on the von Mises yield criterion and assuming $\sigma_z = 0$:

$$2\sqrt{(3)} \tan^{-1}[(\partial_0 - 1)^{\frac{1}{2}}] + \ln \partial_0 - \ln[1 + \sqrt{(3)}(\partial_0 - 1)^{\frac{1}{2}}]^2 + \ln 3W_1^4 - \sqrt{(3)}\,\pi = 0 \tag{5}$$

where $$\partial_0 = \frac{4K^2}{P_0^2}$$

and K = yield stress in simple shear.

For ease of application, this equation may be approximated very accurately by the relationship

$$P_0 = 1.10\, \sigma_y \log W_1 \tag{6}$$

It should be noted, however, that W_1 in Eq. (6) refers to the diameter ratio under pressure which is slightly less than the initial diameter ratio used in Eq. (4). Both equations, then, are in very close agreement and, for calculation purposes, the initial diameter ratio and Eq. (4) will be utilized.

The close agreement of Eq. (6) with the experimental data of Fig. 7 again verifies the assumption of an open end test condition.

Partial Overstrain

In deriving relationships for stresses and strains in a partially overstrained cylinder the following basic assumptions are made.

(*a*) The longitudinal stress throughout the tube is zero.

(*b*) The cylinder is considered infinitely long, since the center portion is far enough from the ends to be free of any end effect. The longitudinal strain, therefore, must be constant with respect to r.

(*c*) The pressure required to produce full plastic flow in the tube is given by Eq. (4), i.e., $P_0 = 1.08\,\sigma_y \log B'$ where B' is the initial diameter ratio.

(*d*) If a cylinder is in the fully plastic condition (subject to an internal pressure P_0) and is then subjected to an external pressure, P_{ex}, in order to maintain the fully plastic condition and equilibrium, the internal pressure, P_{in}, must be increased by an amount equal to P_{ex}.

$$P_{in} = P_0 + P_{ex} \tag{7}$$

1. *Elastic region.* The elastic portion of a partially plastic cylinder is considered as a separate cylinder of internal radius ρ (elastic-plastic interface radius) and external radius b. The radial stress and therefore the internal pressure at ρ is equal to that required to produce elastic breakdown at ρ. Therefore, from Eq. (1):

$$\sigma_{r_\rho} = -\sigma_y \frac{b^2 - \rho^2}{\sqrt{(3b^4 + \rho^4)}} \tag{8}$$

The stresses throughout the elastic region are then obtained from Eq. (8) and the Lamé equations

$$\sigma_{re} = \frac{\sigma_y \rho^2}{\sqrt{(3b^4 + \rho^4)}} \left(1 - \frac{b^2}{r^2}\right) \tag{9}$$

$$\sigma_{te} = \frac{\sigma_y \rho^2}{\sqrt{(3b^4 + \rho^4)}} \left(1 + \frac{b^2}{r^2}\right) \tag{10}$$

where $\rho \leq r \leq b$.

Strains in the elastic region are obtained from the above and the generalized Hookes' law.

$$\epsilon_{re} = \frac{\sigma_y \rho^2}{r^2 E \sqrt{(3b^4 + \rho^4)}} [(1 - \mu) r^2 - (1 + \mu) b^2] \tag{11}$$

$$\epsilon_{te} = \frac{\sigma_y \rho^2}{r^2 E \sqrt{(3b^4 + \rho^4)}} [(1 - \mu) r^2 + (1 + \mu) b^2] \tag{12}$$

$$\epsilon_z = -\frac{2\mu\,\sigma_y\,\rho^2}{E \sqrt{(3b^4 + \rho^4)}} \tag{13}$$

2. *Plastic region.* The plastic portion of the cylinder, i.e. where $a \leq r \leq \rho$, may be considered as a separate, fully plastic cylinder acted on by an internal pressure equal to $-\sigma_{r_\rho}$ at some radius, r, and an external pressure σ_{r_ρ} at ρ. Therefore, from Eq. (7)

$$\sigma_{rp} = \sigma_{r_{\rho'}} + \sigma_{r_\rho} \tag{14}$$

where $\sigma_{r_{\rho'}}$ equals $-P_0$ which is the pressure required to produce full plastic flow in section considered.

From Eq. (4)

$$\sigma_{r_{\rho'}} = 1.08\,\sigma_y \ln \frac{\rho}{r} \tag{15}$$

Substituting σ_{r_ρ} and $\sigma_{r_{\rho'}}$ from Eqs. (8) and (15), respectively, into Eq. (14) yields for the radial stress at radius r in the plastic region.

$$\sigma_{rp} = -\sigma_y \left[1.08 \ln \frac{\rho}{r} - \frac{b^2 - \rho^2}{\sqrt{(3b^4 + \rho^4)}}\right] \tag{16}$$

The well known equilibrium equation for a thick-wall cylinder is

$$\sigma_t = \sigma_r + r \frac{\mathrm{d}\sigma r}{\mathrm{d}r} \tag{17}$$

From Eqs. (16) and (17), the tangential stress in the plastic region is:

$$\sigma_{tp} = \sigma_y \left[-1.08 \ln \frac{\rho}{r} + 1.08 - \frac{b^2 - \rho^2}{\sqrt{(3b^4 + \rho^4)}}\right] \tag{18}$$

The use of the empirical coefficient 1.08 in Eqs. (16) and (18) leads to a slight discontinuity in the σ_t distribution at the elastic-plastic interface. This is due to the coefficient varying somewhat with the elastic-plastic interface location. However, since the error is small, for the sake of simplicity it can be assumed that the coefficient is constant and independent of ρ.

To determine the strains in the plastic region, it is assumed that the only change in volume in the plastic region is elastic in nature and is given by:

$$\epsilon_r + \epsilon_t + \epsilon_z = \frac{1 - 2\mu}{E} (\sigma_r + \sigma_t + \sigma_z) \tag{19}$$

Defining ϵ_r and ϵ_t in terms of radial displacement (u) and substituting values of ϵ_z and σ_r and σ_t from Eqs. (13), (16) and (18) respectively ($\sigma_z = 0$) yields the following differential equation:

$$\frac{\mathrm{d}u}{\mathrm{d}r} + \frac{u}{r} = \frac{\sigma_y}{E}\left\{(1 - 2\mu)\left[2.16 \ln \frac{r}{\rho} + 1.08 - \frac{2(b^2 - \rho^2)}{\sqrt{(3b^4 + \rho^4)}}\right] + \frac{2\mu\rho^2}{\sqrt{(3b^4 + \rho^4)}}\right\} \tag{20}$$

This equation may be solved using the boundary condition of continuity of u at the elastic-plastic interface as given by Eq. (12). The resultant equation for displacement in the plastic region under pressure becomes:

$$\frac{u}{r} = \frac{\sigma_y}{E}\left[1.08(1-2\mu)\ln\frac{r}{\rho} + \frac{\rho^2(1-\mu) - b^2(1-2\mu) + (\rho^2 b^2)/(r^2)(2-\mu)}{\sqrt{(3b^4+\rho^4)}}\right]$$

Pressure-exterior Surface Strain

Graphs of exterior surface strain factor vs. pressure factor were obtained for all specimens tested. All curves for the same diameter ratio were averaged and are shown as the experimental curves in Fig. 9.

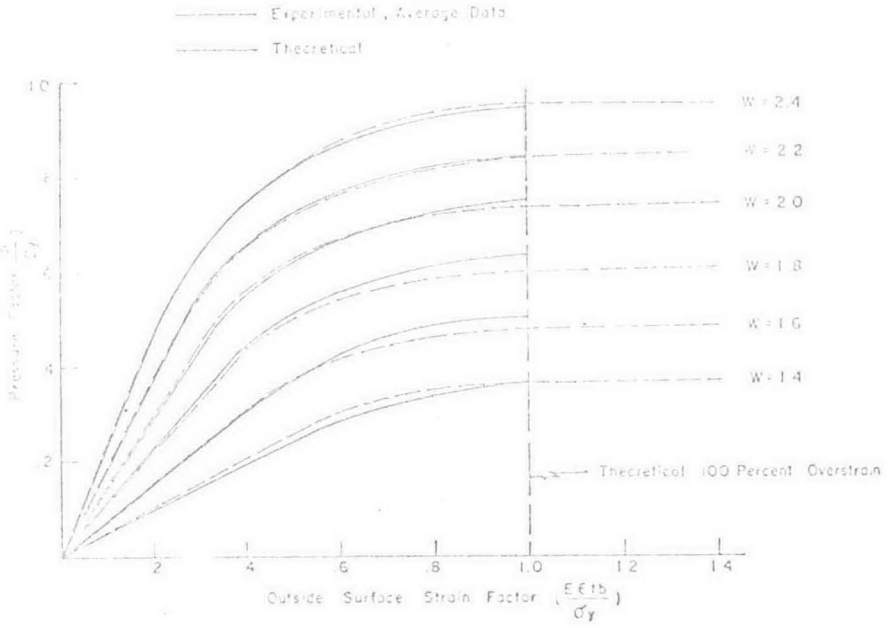

FIG. 9. Pressure factor vs. outside surface strain factor for various diameter ratios.

Since the radial stress at the bore ($r = a$) is equal to the internal pressure, the equation for P_ρ (pressure to produce plastic flow to a depth ρ) may be written from Eq. (16):

$$P_\rho = \sigma_y\left[1.08\ln\frac{\rho}{a} + \frac{b^2-\rho^2}{\sqrt{(3b^4+\rho^4)}}\right] \quad (22)$$

The expression for exterior-surface strain factor is obtained from Eq. (12) by substituting $r = b$

$$SF = \frac{\epsilon_{tb}E}{\sigma_y} = \frac{2\rho^2}{\sqrt{(3b^4+\rho^4)}} \quad (23)$$

Solving Eq. (23) for ρ and substituting in Eq. (22) yields:

$$PF = \frac{1.08}{4}\log\left(\frac{3SF^2W^4}{4-SF^2}\right) + \sqrt{\left(\frac{4-SF^2}{12}\right)} - \frac{SF}{2} \quad (24)$$

Plots of this relationship are shown in Fig. 9 along with the experimental data. As can be seen, very close agreement was obtained between Eq. (24) and the experimental averages.

PERMANENT ENLARGEMENT RATIO

An important factor in the design of thick-wall cylinders using autofrettage is the ratio of the permanent enlargement at the bore to that at the outside

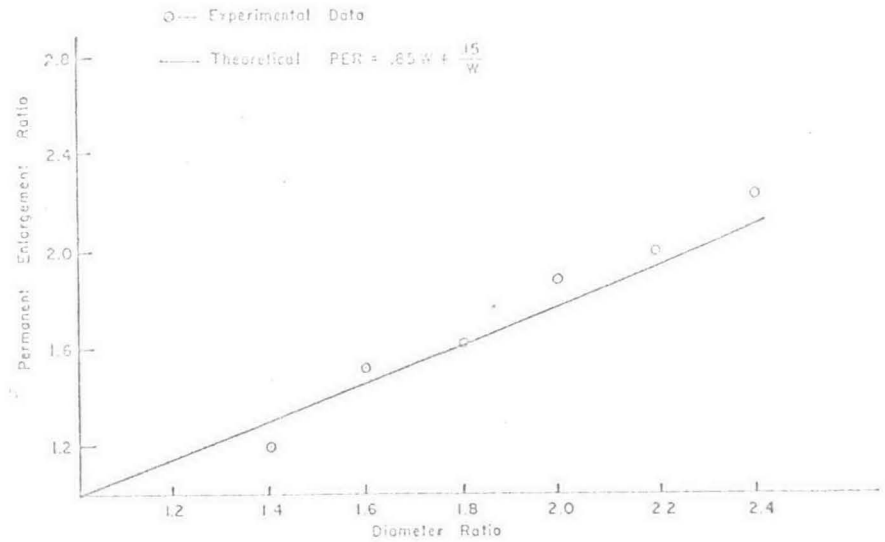

FIG. 10. Permanent enlargement ratio vs. diameter ratio.

surface. This ratio was obtained by physical measurements for all specimens tested. No correlation was found between permanent enlargement ratio and percent bore enlargement and therefore, all values for the same diameter ratio were averaged. These averaged values are shown as experimental points in Fig. 10.

The theoretical relationship for permanent enlargement ratio may be derived as follows. The enlargement of the bore under pressure is given by Eq. (21) substituting $r = a$. To find the permanent enlargement of the bore, the elastic recovery must be substracted from the enlargement under pressure. The elastic recovery is given by the Lamé equation and the value of pressure from Eq. (22).

The enlargement of the outside surface under internal pressure is found from Eq. (12), letting $r = b$ and the elastic recovery of the exterior surface is again subtracted as was that for the inside surface. Dividing the resulting equation for permanent bore enlargement by that for permanent enlargement of the outside surface yields the following equation for the permanent enlargement ratio.

$$PER = \frac{1}{2}\left[(2-\mu)\,W + \frac{\mu}{W}\right] \qquad (25)$$

A plot of this equation is shown in Fig. 10 for $\mu = 0.3$.

It is interesting to note that Eq. (25) can be derived directly from geometric considerations assuming no net change in volume as a result of overstrain.

Percent Permanent Bore Enlargement

From Fig. 9 it can be seen that, when a condition of 100 percent overstrain (strain factor = 1.0) is reached, the pressure-strain curve becomes essentially flat. It is, therefore, assumed that no additional benefit can be obtained by further deformation and that 100 percent overstrain is the optimum amount of deformation. Actually, for higher diameter ratios where reverse yielding will occur at the bore because of the 100 percent overstrain pressure, the optimum percent bore enlargement may be slightly less. However, in the diameter ratios investigated, this reverse yielding effect is considered negligible.

The permanent bore enlargement required to produce 100 percent overstrain was determined experimentally by plotting the maximum exterior surface strain factor vs. the percent permanent bore enlargement obtained for each cylinder. This yielded a family of curves, one for each diameter ratio. The point of intersection of each of these curves with the horizontal line representing a strain factor of 1.0 indicated the value of permanent bore enlargement to just produce 100 percent overstrain. These points are plotted in Fig. 11.

The theoretical curve shown is obtained by substituting $r = a$ and $\rho = b$ in Eq. (21) yielding the following equation for bore strain at 100 percent overstrain pressure.

$$\epsilon_{tac} = \frac{\sigma_y}{E}\left[-1.08(1-2\mu)\ln W + \frac{\mu}{2} + \left(\frac{2-\mu}{2}\right)W^2\right] \qquad (26)$$

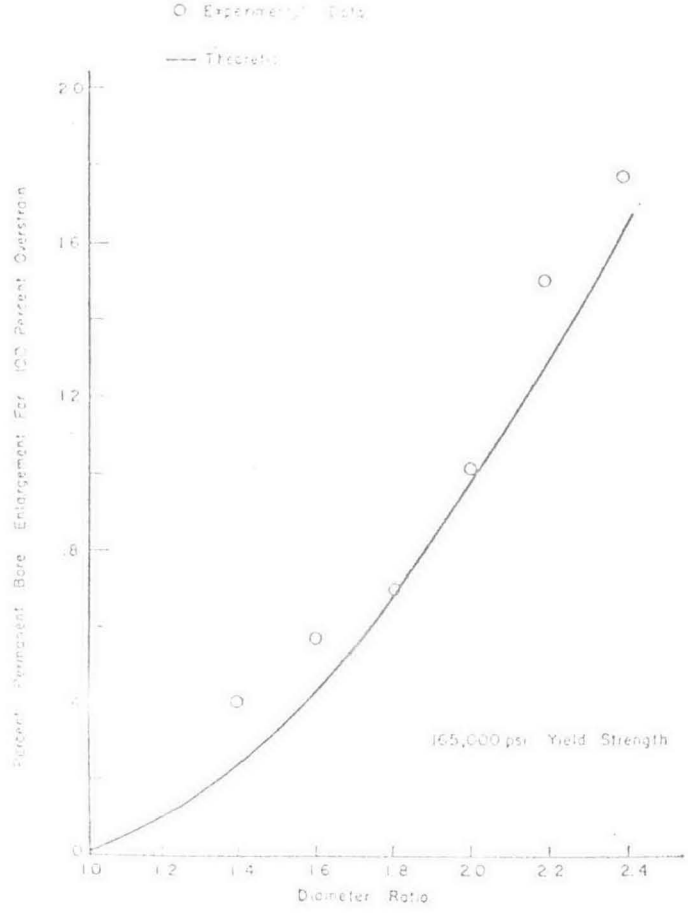

FIG. 11. Percent permanent bore enlargement for 100 per cent overstrain vs. diameter ratio.

The elastic recovery at the bore is given by the Lamé equations and Eq. (4).

$$\epsilon_{tae} = \frac{\sigma_y}{E}\,\frac{1.08\ln W}{W^2-1}\,[(1+\mu)\,W^2 + (1-\mu)] \qquad (27)$$

Subtracting Eq. (27) from Eq. (26) yields:

$$\epsilon_{taperm} = [\mu + (2-\mu)W^2]\left[\frac{1}{2} - \frac{1.08\ln W}{W^2-1}\right] \qquad (28)$$

This equation is plotted in Fig. 11 for $\mu = 0.3$ and is in good agreement with the experimental values.